Materials Science & Engineering A 733 (2018) 128–136

Contents lists available at ScienceDirect

Materials Science & Engineering A

journal homepage: www.elsevier.com/locate/msea

# High-cycle fatigue behavior of 18Cr-8Ni austenitic stainless steels with grains ranging from nano/ultrafine-size to coarse

J. Liu, X.T. Deng*, L. Huang, Z.D. Wang

*State Key Laboratory of Rolling and Automation, Northeastern University, Shenyang 110819, China*

ARTICLE INFO

*Keywords:*
Austenitic stainless steel
Grain size refinement
Strain-induced martensite
Fatigue behavior

ABSTRACT

The effect of grain size on high-cycle fatigue behavior under axial forces in the 18Cr-8Ni austenitic stainless steel was investigated. The fatigue strength of the austenitic stainless steel, obtained by the phase reversion process, with grain sizes of 400 nm, 1.4 μm, and 12 μm were 811 MPa, 568 MPa, and 501 MPa, respectively. After cyclic deformation, remarkable slip bands were formed on the surfaces of coarse-grained (CG) and fine grained (FG) samples, whereas, no slip bands or other deformation marks were observed on the surface of the nanograined/ultrafine-grained (NG/UFG) sample. Randomly oriented cracks of a few micrometers long appeared on the CG sample, while the cracks on NG/UFG were larger and the propagation direction was perpendicular to the loading direction. The increase in hardness after cycling was inversely proportional to the increase in strain-induced martensite among the NG/UFG, FG, and CG samples. Strain-induced martensite was produced primarily at the grain boundaries or slip bands in CG steels; in contrast, martensite was concentrated in the vicinity of nanograins in FG and NG/UFG steels. After fatigue, in the CG sample, a small amount of martensite, deformation bands, and large number of dislocations were formed, while in the NG/UFG sample a very small amount of ε-martensite, strain-induced martensite, and dislocations were formed.

## 1. Introduction

Improving the strength of an austenitic stainless steel without sacrificing its good ductility to meet various application requirements has recently become a research area of interest. In the past, researchers adopted severe plastic deformation (SPD) methods to refine grain size, such as equal channel angular processing (ECAP), accumulative roll-bonding (ARB), and high-pressure torsion (HPT) [1–3]. Recently, one of the most effective processing routes to NG/UFG stainless steels, called the strain-induced martensite reversion process, was proposed by Misra's group [4–7]. Metastable stainless steels, such as types 301, 304, and 316 L, with nano/ultrafine grain (NG/UFG) structures, have been obtained by this technique; these steels, possess a highly useful combination of static mechanical strength and ductility [8–11]. The deformation behavior under monotonic loading of austenitic stainless steels with grain sizes ranging from nano/ultrafine to coarse has been extensively investigated to understand the deformation mechanisms responsible for their tensile strength–ductility combinations [7,12–14]. These studies show that as the grain size increases from NG/UFG to CG, the deformation mechanism changes from nanoscale twinning to strain-induced martensite, which is related to the increased stability of austenite with a decrease in grain size [12].

To enable the use of NG/UFG materials in modern and future industrial applications, it is necessary to understand the deformation mechanism not only under monotonic loading, but also under cyclic loading. The fatigue strength of the materials is closely related to their tensile strength. Numerous investigations of pure metals and light alloys have shown that fatigue resistance can be greatly improved by grain refinement during stress-controlled cyclic loading [15–19]. This is because a high strength can effectively inhibit the generation of cracks, which is related to the fact that fine grains can act as obstacles to dislocation movement [20,21]. However, high strength apparently has deleterious effects on the crack propagation rate because of the different crack paths, related to the lack of ductility [18,19].

Di Schino et al. [22] employed a strain-induced martensite treatment method to obtain an AISI 304 stainless steel having grain sizes 1–47 μm, and the fatigue test results showed a strong improvement in fatigue resistance with grain refinement. Hamada et al. [23] studied the high-cycle bending fatigue behavior of UFG and CG 301LN austenitic stainless steels, and the results also showed that the fatigue limit was significantly increased with grain refinement. Further investigation revealed fatigue cracking along the grain boundaries and the formation of extended persistent slip band-like shear bands (SBs) in the UFG structure, while slip bands and strain-induced martensite plates were

* Corresponding author.
*E-mail address:* dengxiangtao123@163.com (X.T. Deng).

https://doi.org/10.1016/j.msea.2018.07.043
Received 11 April 2018; Received in revised form 6 July 2018; Accepted 12 July 2018

found in the CG structure [24]. Järvenpää et al. [25] carried out axial tension–tension fatigue experiments on the 301LN austenitic stainless steel (with various grain sizes, from submicron to coarse); the results indicated that during the first cycles, cyclic hardening is very fast and pronounced, and a high fraction of α´-martensite is formed in both the UFG and CG structures.

Even though studies on cyclic deformation behavior of austenitic stainless steel have been performed, as mentioned above, there have been few studies on this behavior under an axial force. Furthermore, there are still some confusions regarding the cyclic stability and microstructure evolution in the high-cycle fatigue processes of NG/UFG structure. In the present paper, an extended study is presented to obtain more experimental data and create better understanding on the fatigue behavior of phase reversion annealed NG/UFG austenitic stainless steel. An attempt was made to illustrate the damage behavior and the evolution of strain-induced martensite of NG/UFG structure under axial tension–tension cyclic loading condition, and compare them with the behavior of CG and UFG austenitic stainless steels.

## 2. Material and experimental procedure

The experimental material considered was a commercial 18Cr-8Ni austenitic stainless steel. The steel strips had an initial thickness of 4.5 mm, and their nominal compositions (weight percent) are given in Table 1. Strips with dimensions 100 mm × 250 mm were cut from a sheet and cold rolled in a laboratory rolling mill until 70% reduction was achieved at room temperature. The final thickness of the experimental steel was ~ 1.3 mm, where a reduction of 0.12 mm was carried out in each pass. The samples were then annealed under conditions of 710 °C-10 min, 760 °C-5 min, and 950 °C-5 min in a resistance furnace to obtain the NG/UFG to CG austenite structures.

The tensile properties were obtained using a SANS micro-force testing system. Longitudinal tensile test specimens were prepared in accordance with the ASTM E8-04 standard, with a gage length of 25 mm and width of 6.25 mm. All tensile tests were conducted at room temperature using a crosshead speed of 3 mm/min.

Axial tension–tension high-cycle fatigue tests were conducted using a GPS100 digital high-frequency fatigue testing machine at ambient temperature. The applied stress ratio was $R = 0.2$, and the cycling frequency was approximately 95 Hz. The load axis of hourglass-shaped test specimens was along the rolling direction, and the dimensions were as shown in Fig. 1. Before fatigue tests, all specimens were ground to remove surface defects and then electro-polished using a mixed solution of 8% perchloric acid and 92% alcohol to obtain a strain-free and mirror-like finish for microscopy observation.

The microstructures before and after fatigue were examined with a Zeiss Ultra 55 scanning electron microscope (SEM) equipped with an electron backscatter diffraction (EBSD) unit. For the EBSD study, samples were prepared by electropolishing in a solution of 8% perchloric acid and alcohol at a potential of 22 V for 20 s. The strain-induced martensite and reversed austenite phase identifications were performed using X-ray diffraction (XRD) with Cu Kα radiation. A quantitative estimate of the phase volume fraction was determined using the following equation:

$$V_A = \frac{1/n\sum_{j=1}^{n}\frac{I_A^j}{R_A^j}}{1/n\sum_{j=1}^{n}\frac{I_A^j}{R_A^j} + 1/n\sum_{j=1}^{n}\frac{I_M^j}{R_M^j}} \tag{1}$$

**Table 1**
Chemical composition of the investigated steel samples (wt%).

| Steel | C | Si | Mn | Cr | Ni | Cu | N | Fe |
|---|---|---|---|---|---|---|---|---|
| 18Cr-8Ni | 0.04 | 0.39 | 1.09 | 17.94 | 7.92 | 0.0379 | 0.0470 | Balance |

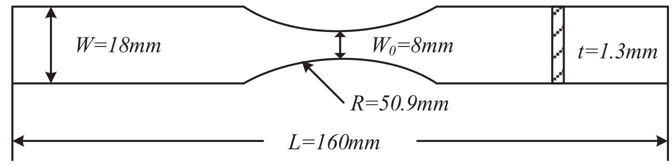


**Fig. 1.** Shape and dimensions of fatigue specimens.

where n is the number of peaks examined, $R_M$ and $R_A$ are the relative intensities of the three (*hkl*) plane selected reflections of α′ and γ phases, and $I_M$ and $I_A$ are the integrated intensities of the corresponding phases.

## 3. Results

### 3.1. Initial microstructures

The grain size of the as-received 18Cr-8Ni austenitic stainless steel with a fully austenitic structure is 24 µm. In this study, the grain size was refined by severe cold deformation, with 70% reduction and subsequent annealing at 710 °C-10 min, 760 °C-5 min, and 950 °C-5 min. The structures of the annealed samples under various annealing conditions are presented in Fig. 2. It can be seen that annealing at 710 °C for 10 min (Fig. 2a) resulted in the smallest average grain size, of approximately 400 nm, and involved a mixture of nanoscale and microscale grains. After annealing at 760 °C for 5 min, as shown in Fig. 2b, the average grain size increased to 1.4 µm; however, nanoscale grains also existed. Fig. 2c shows that the largest average grain size of approximately 12 µm was obtained by annealing at 950 °C for 5 min, and the distribution was more uniform than that for the grain sizes of 400 nm and 1.4 µm. The average grain sizes of 400 nm, 1.4 µm, and 12 µm are referred to here as nanograined/ultrafine-grained (NG/UFG), fine-grained (FG), and coarse-grained (CG), respectively.

### 3.2. Mechanical properties

The tensile engineering stress-strain curves of the NG/UFG, FG, and CG steels are displayed in Fig. 3. The CG steel has a relatively low yield stress (316 MPa) and very high ductility (70%). As the grain size decreases, the yield strength increases and the elongation of the samples decreases. For the grain size of 1.4 µm (FG), the yield stress increased to 571 MPa and the elongation was 51.7%. NG/UFG steel revealed a high yield stress of 878 MPa, more than two times that of the CG steel, as well as an acceptable elongation of 32.9%.

### 3.3. Fatigue strength

Fig. 4 shows the relationship between the peak stress and fatigue life for CG, FG, and NG/UFG steels. When the materials can cycle a sufficiently high number of cycles, such as $10^7$, without failure, the stress value is defined as the fatigue limit. It can be seen from Fig. 4 that the fatigue limit decreased with increasing grain size, in agreement with previous studies [22,23,25]. The corresponding fatigue limits were 501 MPa, 568 MPa, and 811 MPa for CG, FG, and NG/UFG steels, respectively. For NG/UFG steel, the fatigue limit (811 MPa) was lower than the yield stress (878 MPa), and the two values for FG were very close. However, for the CG steel, the fatigue limit (501 MPa) was much higher than the yield strength (316 MPa).

### 3.4. Cycling damage behavior

Fig. 5a–c show the fracture-side surface morphologies of the CG, FG, and NG/UFG samples, and Fig. 5d–f are the corresponding local amplification figures. The surface of the CG sample (with a fatigue life of $6.4 \times 10^4$ cycles) was quite uneven (Fig. 5a), and intrusions and